REVIEW ARTICLES | FOCUS
PUBLISHED ONLINE: 30 NOVEMBER 2009 | DOI: 10.1038/NPHOTON.2009.231
nature photonics

Optical quantum memory

Alexander I. Lvovsky*, Barry C. Sanders and Wolfgang Tittel

Quantum memory is essential for the development of many devices in quantum information processing, including a synchronization tool that matches various processes within a quantum computer, an identity quantum gate that leaves any state unchanged, and a mechanism to convert heralded photons to on-demand photons. In addition to quantum computing, quantum memory will be instrumental for implementing long-distance quantum communication using quantum repeaters. The importance of this basic quantum gate is exemplified by the multitude of optical quantum memory mechanisms being studied, such as optical delay lines, cavities and electromagnetically induced transparency, as well as schemes that rely on photon echoes and the off-resonant Faraday interaction. Here, we report on state-of-the-art developments in the field of optical quantum memory, establish criteria for successful quantum memory and detail current performance levels.

Quantum information science incorporates quantum principles into information processing and communication. Among the most spectacular discoveries and conjectures are quantum cryptography, which we know can allow the secure communication of information through public channels[1], and quantum computing, which may be able to efficiently solve certain computational problems believed to be intractable by classical computing[2]. Furthermore, quantum computers allow the efficient simulation of quantum dynamics[3]. The prototypical model of quantum information processing represents information as strings of qubits, and performs processing using unitary quantum gates.

A qubit is a single-particle state in a two-dimensional Hilbert space. If the particle is a single photon, then the qubit can be encoded in several ways. For example, in polarization encoding the logical states $|0\rangle$ and $|1\rangle$ can correspond to a single photon being left- and right-circularly polarized, respectively. Other examples include path[4], photon-number[5,6] and time-bin encodings[7]. A general qubit state can be expressed as a superposition of the states $|0\rangle$ and $|1\rangle$, and general states of quantum information are superpositions of strings of qubits. Quantum memory must be able to store qubit strings (or parts of qubit strings) faithfully, and release them on demand.

Storage of a quantum state, however, does not need to be perfect. Fault-tolerant quantum error correction can be utilized to allow sufficient operation of an imperfect memory, as long as the fidelity of the memory 'gate' exceeds a particular performance threshold[8,9]. It is instructive, therefore, to study the specific requirements of optical quantum memory for quantum information tasks.

Performance criteria

In general, quantum memory stores a pure or mixed state represented by a density matrix ρ, and outputs a state ρ', which should be close to ρ. The ultimate performance criterion for quantum memory is the lowest (worst-case) fidelity with respect to the set of input states, where the storage fidelity for a specific state is given by

$$F(\rho) = \mathrm{Tr}\sqrt{\sqrt{\rho'}\rho\sqrt{\rho'}}$$

Hence there exists a threshold worst-case fidelity, beyond which fault-tolerant quantum error correction methods can overcome memory imperfection[8,9].

The fidelity of quantum optical memory for an arbitrary set of input states can be determined by characterizing it as a quantum process[10,11]. However, this procedure is relatively bulky, so in practical experimental implementations other performance criteria are used. For example, 'fidelity' sometimes refers to state a overlap $\langle\psi|\rho'|\psi\rangle$ (possibly after post-selection), which is the square of $F(\rho)$ for the case when $\rho = |\psi\rangle\langle\psi|$ is a pure state. 'Average fidelity' is also often used, in which the average is taken over all input states with respect to an assumed prior distribution[12].

Another popular criterion is the efficiency η, which is the ratio between the energies of the stored and retrieved pulses. Efficiency, although easy to determine experimentally, does not account for possible detrimental effects such as contamination of the retrieved state by excess noise from the storage medium.

The multimode capacity of a quantum memory determines the number of optical modes that can be stored in a memory cell with a performance above the requisite performance threshold. The multimode capacity strongly depends on the memory mechanism[13,14].

Quantum memory must be able to store a state long enough to perform a particular task, so storage time is another essential criterion for memory performance. For many applications, an appropriate 'figure of merit' would be the delay–bandwidth product, the ratio between the storage time and duration of the stored pulse.

Applications

In optical quantum computation, the role of a quantum memory is to store quantum bits such that operations can be timed appropriately. Many qubits are processed in parallel at each 'step' in time, and these processing steps must be synchronized[4,15,16].

Quantum communication suffers from imperfect transmission channels, making quantum key distribution possible only over finite distances. The quantum repeater[17,18] solves this problem and permits quantum communication over arbitrary distances, with a polynomial resource cost that is a function of the distance. A necessary component of the quantum repeater is quantum memory, which, similar to quantum computation, allows synchronization between entangled resources distributed over adjacent sections of the transmission link.

Furthermore, quantum memory for light also has applications in precision measurements based on the quantum interference of atomic ensembles. By transferring quantum properties of an optical state to the atoms, the quantum noise level of the measured observable can be reduced, thereby improving the precision of magnetometry, clocks and spectroscopy[19].

Finally, quantum optical memory can be used as a component of single-photon sources. If a single-photon detector is placed in one of the emission channels of non-degenerate spontaneous parametric down-conversion, a detection event indicates emission of a photon pair, and thus the presence of a single photon in the other channel[20,21]. Such a heralded photon is emitted at an arbitrary time,

Institute for Quantum Information Science, University of Calgary, Alberta T2N 1N4, Canada. *e-mail: lvov@ucalgary.ca

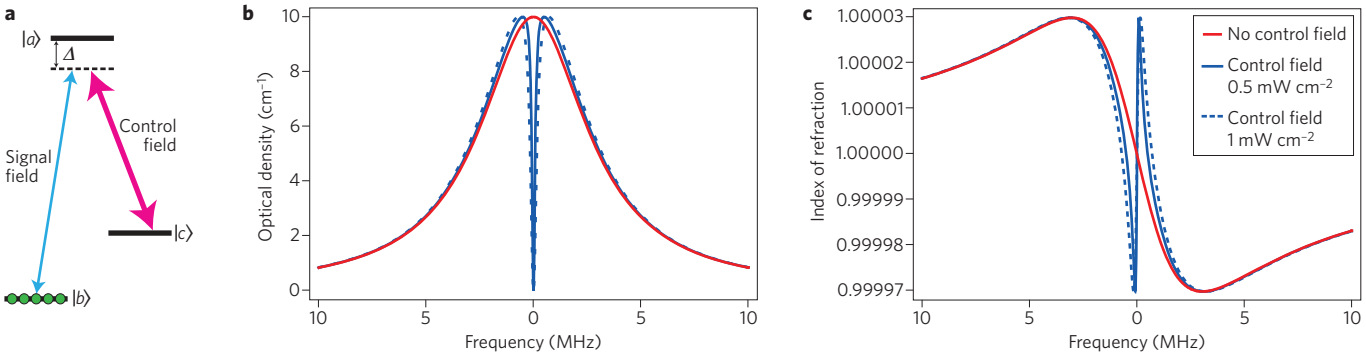

Figure 1 | Electromagnetically induced transparency. a, Atomic level configuration. Both fields are detuned by Δ from resonance by the same frequency such that the two-photon resonance condition is fulfilled. **b**,**c**, Plots showing the behaviour of optical density (**b**) and the index of refraction (**c**) around the resonant frequency, for an ensemble of atoms with (blue) and without (red) EIT. Despite a significant optical depth, the variation in the index of refraction is very small. The atomic parameters used to generate the plots correspond to a cloud of ultracold rubidium atoms.

however, making it unsuitable for many applications. Despite this, a heralded photon can be placed in a quantum memory cell and released when needed, effectively implementing an on-demand source of single photons.

Below we review recent theoretical and experimental work on the different approaches to quantum memory.

Optical delay lines and cavities

The simplest approach to storing light is an optical delay line, such as an optical fibre. This approach has been used to synchronize photons with the occurrence of certain events[22]. However, the storage half-time — the time after which half the photons are lost — is limited to around 70 μs when using 1.5-μm wavelength photons in telecommunications fibres, which corresponds to a fibre length of around 15 km. The half-time decreases at other wavelengths due to increased loss. Furthermore, the storage time of an optical delay is fixed by the delay length — this is unsuitable for most applications because a variable, on-demand output is required.

Alternatively, light can be stored in a high-Q cavity. The light cycles back and forth between the reflecting boundaries, allowing it to be injected into and retrieved from the cavity through electro-optical or nonlinear optical means[23–25], or by transferring the quantum state to passing atoms[26]. For example, light has been stored for over a nanosecond in wavelength-scale photonic crystal cavities that have a tunable Q factor, thus allowing control over the storage time[27]. Dynamic control of Q can be achieved by adiabatically tuning the frequency of the stored light, yielding output pulses as short as ~0.06 ns — much shorter than the storage time[28].

Unfortunately, the storage of light in cavities suffers from a trade-off between short cycle time and long storage time, which limits the efficiency. Therefore, whereas optical delay lines and nanocavities could be appropriate for obtaining on-demand single photons from heralded sources[20,21], they may not be suitable for quantum memory or quantum repeaters.

Electromagnetically induced transparency

Electromagnetically induced transparency (EIT) is a nonlinear optical phenomenon observed in atoms that have an energy level structure resembling the letter Λ (Fig. 1a). Two optical fields — the weak signal field, which carries the quantum information, and the strong control field, which is used to 'steer' the atomic system — couple the excited level to their respective ground levels.

If the control field is absent, the signal field, which interacts with the resonant two-level system, undergoes partial or complete absorption. If the control field is present, however, the absorption of the signal is greatly reduced whenever the frequency difference of the two optical fields is close to the frequency of the Raman transition between the ground states of the system (known as two-photon resonance; Fig. 1b).

EIT is largely insensitive to the detuning Δ of the optical fields from their respective individual transitions. It can therefore exist in the presence of inhomogeneous broadening as long as both optical transitions experience the same frequency shift. A good example is a Doppler-broadened warm atomic gas, provided that the ground levels are of similar energies and the two optical fields are co-propagating. Counter-intuitively, the EIT window in this case is narrower than in the case of purely homogeneous broadening[29].

Slow light and memory. According to the Kramers–Kronig relations, an anomaly in the absorption spectrum is always accompanied by an anomaly in dispersion. In the case of EIT, the signal field experiences large normal dispersion (Fig. 1c), which implies reduction of the group velocity by a factor inversely proportional to the intensity of the control field[30,31]. Experiments have shown a slowdown of up to seven orders in magnitude[32,33].

This slowdown can serve as a basis for quantum memory (Fig. 2a). A light pulse, resonant with the EIT window, enters the EIT medium and slows down. This involves spatial compression, so the pulse — whose initial spatial extent by far exceeds the medium length L — will fit inside the medium. When the pulse is inside, the control field is adiabatically decreased, reducing the group velocity to zero and thereby 'collapsing' the EIT window and storing the pulse in the medium. When the pulse needs to be retrieved, the control field is turned back on. The pulse then resumes its propagation and leaves the EIT medium[31,34–36].

Before the arrival of the signal pulse, all atoms are optically pumped by the control field into the ground level $|b\rangle$, giving an initial atomic state of $|\psi_0\rangle = |b_1 \ldots b_N\rangle$. When the signal is stored, its quantum state is transferred to a collective excitation of the atoms in the EIT medium. For example, if the signal state is a single photon, the atomic state becomes (neglecting normalization)

$$|\psi_1\rangle = \sum_j \psi_j e^{i\Delta k z_j} |b_1 \ldots c_j \ldots b_N\rangle \qquad (1)$$

where N is the number of atoms in the ensemble, z_j is the position of atom j along the field propagation and Δk is the difference in wavevectors of the control and signal fields. In other words, one of the atoms is transferred to the other ground-state, $|c\rangle$, but it is not known which atom is transferred.

In the ideal case of absent ground state decoherence, the atomic state does not contain any fraction of the excited state $|a\rangle$ during both

NATURE PHOTONICS DOI: 10.1038/NPHOTON.2009.231

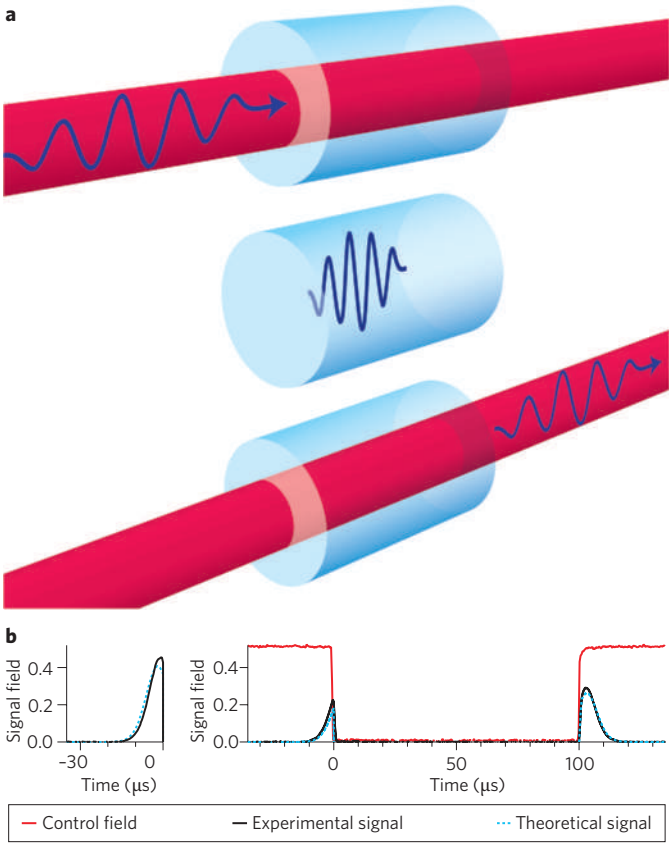

Figure 2 | Storage of light by electromagnetically induced transparency. **a**, Idealized schematic. The signal pulse enters the cell under EIT conditions when the control field is switched on (top). The control field is then switched off while the spatially compressed pulse propagates inside the EIT cell, allowing the quantum information carried by the pulse to be stored as a collective excitation of the ground states (middle). When the pulse needs to be retrieved, the control field is switched on again and the pulse exits the cell (bottom). **b**, Optimized classical light storage in a rubidium vapour cell (αL = 24) with a buffer gas, showing an input signal pulse of optimal shape (left), and storage and retrieval of the pulse (right). Because of the finite optical depth, the signal pulse does not entirely fit into the cell, resulting in a fraction of the pulse leaking through the cell before the control field is turned off. Part **b** reproduced with permission from ref. 40, © 2008 APS.

the transfer and storage periods. This means that EIT-based memory is not affected by the spontaneous decay of this state.

In 2001, the first experimental demonstrations of EIT-based light storage were reported[37,38]. In the study of Phillips *et al.*[37], macroscopic 10–30-μs pulses at a wavelength of 795 nm were stored in a 4-cm rubidium vapour cell for up to 0.2 ms. Liu *et al.*[38] magnetically trapped a thermal cloud of sodium atoms to achieve a memory decay time of 0.9 ms, and in this study the verification of memory performance involved measuring the intensity of the stored and retrieved pulses.

Gorshkov *et al.*[39] developed a detailed theory of the EIT-based storage of light for a variety of experimental configurations, which has provided techniques for optimizing memory performance. In the case of optimal matching of the temporal shapes of the input signal and control fields, the optical depth αL (where α is the absorption index) of the storage medium outside the EIT window is the only parameter that determines the storage efficiency. For efficient storage, αL must be significantly greater than one.

This requirement can be understood as follows. First, the spectrum of the signal pulse must fit within the transparency window, thus imposing a lower bound on the signal pulse duration. Second, the pulse must fit geometrically within the EIT medium; the spatial extent of the signal pulse, compressed as a result of the slow-light effect, must not exceed L, thus setting an upper bound on the signal pulse duration. These bounds can be satisfied at the same time if the slowdown is sufficient, which requires the contrast in the EIT window — and therefore αL — to be high. Fulfilling this requirement is a challenge in many optical arrangements, including in magneto-optical traps and solid-state systems.

The findings of Gorshkov *et al.* were verified in an experiment involving warm rubidium vapour. For moderate optical densities ($\alpha L \lesssim 25$), the experimental results showed excellent agreement with a three-level theoretical model that has no free parameters[40–42] (Fig. 2b). For higher optical densities, four-wave mixing effects become important, leading to the generation of an additional (idler) optical mode. Although the associated parametric gain may lead to better compression of the pulse[43], it also introduces additional quantum noise that degrades the storage fidelity.

EIT-based memory can be implemented in solid media, which has advantage of significantly longer storage times. Following initial observations of EIT[44], and ultraslow and stored light[45] in praseodymium-doped Y_2SiO_5 crystals, Longdell *et al.* stored light in a similar crystal with a decay time of 2.3 s (ref. 46). A disadvantage of this crystal in light-storage applications is its relatively low optical density, which results from the inhomogeneous broadening associated with the difference in ionic radii of Y^{3+} and Pr^{3+}. Attempts to increase the dopant concentration only result in a broader line without increasing the optical density. Recently, EIT has been observed in Pr^{3+}:$La_2(WO_4)_3$ (another praseodymium-doped crystal), which exhibits an inhomogeneous broadening that is 15 times smaller than Pr^{3+}:Y_2SiO_5 but has significantly increased homogeneous decay[47].

We now review a few experiments in which quantum states of light have been stored and retrieved, with the retrieved pulses retaining some of their non-classical properties. In 2005, single photons generated using the DLCZ protocol (see below) were stored in a cold atom cloud[48] and a vapour cell[49], and retrieved approximately 0.5 μs later. Sub-Poissonian statistics of the retrieved light were verified using a Hanbury Brown and Twiss detection scheme. In an important step towards real-world applications, a dual-rail single-photon qubit was stored in two ultracold atomic clouds[50].

In 2004, propagation of another quantum information primitive, the squeezed vacuum state, was observed under EIT conditions[51], and in 2008 this was followed by experimental demonstrations of the storage of squeezed vacuum states[52–54]. Quadrature noise of the retrieved pulses was measured by means of homodyne detection and observed to be below the shot noise level, demonstrating that some of the initial squeezing was preserved through the storage procedure.

EIT-based storage of quantum light suffers from background noise in the retrieved signal. This noise is likely to originate from the repopulation of the state $|c\rangle$ (ref. 55) associated, for example, with the atomic drift in and out of the interaction area. In the presence of the control field, the atoms are pumped from $|c\rangle$ to the excited state $|a\rangle$, after which they spontaneously decay back to the ground state and emit thermal photons, which contaminate the signal mode. This effect is negligible when a macroscopic pulse is stored and its classical properties (such as the energy and the pulse shape) are measured on retrieval. On the other hand, the detrimental effects of noise become significant when the quantum properties of the storage process are of interest. To minimize noise therefore, most experiments investigating non-classical light storage compromise on storage efficiency and lifetime.

Background noise has been observed in a homodyne detection setting[56] and investigated theoretically[57–59], and these predictions

were successfully reproduced in an experiment involving the propagation of squeezed light under EIT conditions[60]. Unlike the classical case, however, so far there has been no comprehensive study involving a full, experimentally verified theoretical quantum description of EIT-based light storage.

The DLCZ protocol

Closely related to EIT-based quantum memory is a scheme proposed by Duan, Lukin, Cirac and Zoller (DLCZ) for creating long-lived, long-distance entanglement between atomic ensembles[61]. An elementary step of the DLCZ procedure consists of creating a stored collective excitation of the type given in equation (1) in an ensemble of Λ-type atoms. In contrast with regular optical memory, this excitation is produced not by an external photon entering an ensemble but by the ensemble itself interacting with a classical (write) optical field, and is heralded by emission of an idler photon (Fig. 3a). This excitation can be retrieved in the form of a signal photon by applying a control (read) field to the ensemble (Fig. 3b) after the required storage period has elapsed.

In many ways, the DLCZ protocol resembles heralded preparation of a single photon from a pair of photons generated through parametric down-conversion[20,21]. A fundamental difference is that the heralded atomic excitation is long-lived and can be retrieved at an arbitrary time, which enables its application in a quantum repeater. The protocol can also be viewed as a deterministic single-photon 'pistol': when it is 'loaded' with an idler detection event, it can 'shoot' the signal photon on demand.

Figure 3c illustrates the preparation of a single link of long-distance entanglement between two remote atomic ensembles. The ensembles are simultaneously illuminated with write pulses and the spatial modes in which the idler photon is to be detected are mixed at a beamsplitter. If a photon has been detected in one of the beamsplitter outputs then it is impossible to tell which of the two ensembles has emitted the photon. As a result, the state of the two ensembles becomes an entangled superposition $|\psi\rangle = (|\psi_0\rangle|\psi_1\rangle + e^{i\varphi}|\psi_1\rangle|\psi_0\rangle)/\sqrt{2}$, where the phase φ depends on the lengths of the optical links between the ensembles and the detection apparatus.

The DLCZ scheme is ideally suited for quantum repeater applications, but does not directly enable storage of arbitrary quantum information from outside the system. In principle, arbitrary qubits can be stored in an atomic ensemble using the DLCZ scheme through quantum teleportation[62]. However, because the atom–light entanglement is generated by spontaneous emission, an optical quantum memory is only useful in a post-selected way.

There has been a significant amount of experimental work on applying the DLCZ protocol to quantum repeaters. Such detail is beyond the scope of this review, but has been summarized elsewhere[18].

Photon-echo quantum memory

Photon-echo quantum memory relies on transferring the quantum state carried by an optical pulse to a collective atomic excitation, which is similar in principle to EIT-based storage schemes. In contrast to EIT, however, photon-echo quantum memory takes advantage of inhomogeneous broadening. Consider again an ensemble of two-level atoms in the state $|\psi_1\rangle$. After absorption of a signal photon at $t = 0$, the state is given, in an un-normalized form, by[13]

$$|\psi_1\rangle = \sum_j \psi_j e^{-i\delta_j t} e^{ikz_j} |b_1 \ldots a_j \ldots b_N\rangle$$

where k denotes the wavevector of the signal field, δ_j is the transition detuning of atom j with respect to the light carrier frequency, and all other variables are as previously defined. Although the atomic dipoles are initially phase-aligned with k, this alignment rapidly decays because δ_j differs for each atom.

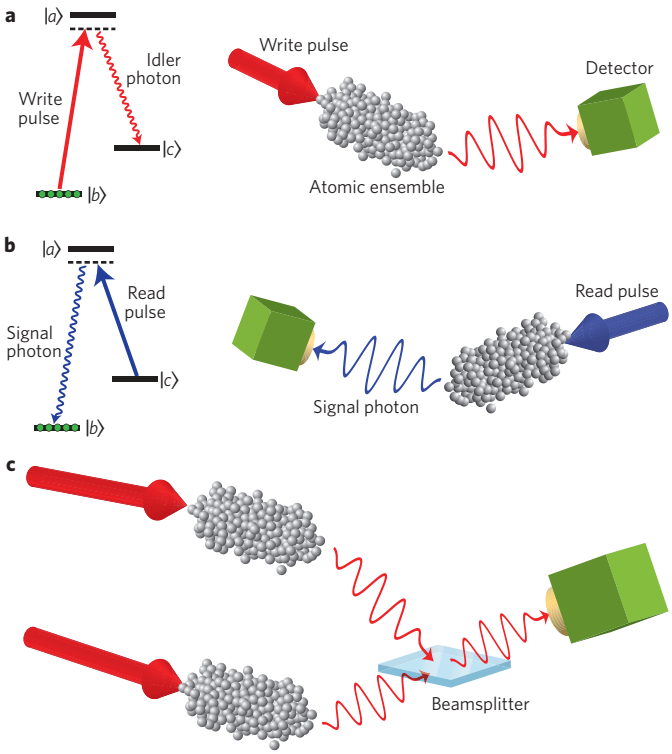

Figure 3 | The DLCZ protocol. a, Atoms initially in the state $|b\rangle$ are illuminated with a weak off-resonant 'write' pulse, allowing some atoms to Raman transfer to the state $|c\rangle$. Each transfer is associated with the scattering of a photon in an arbitrary direction. A single spatial mode of the scattered (idler) light is selected, for example, by means of an optical fibre, and is measured using a single-photon detector. The parameters of the write pulse are chosen such that the probability of a detection event is low. If such an event does occur, it indicates with high likelihood that exactly one photon has been emitted by the atomic ensemble into the detection mode. Spatial filtering erases the information about the location of the atom that emitted the photon and, as a result, the detection event projects the atoms onto a collective superposition of the type given in equation (1). **b**, Application of a classical 'read' pulse converts this collective excitation to an optical form, resulting in the emission of a signal photon and the transfer of atoms back to the state $|b\rangle$. **c**, Entanglement between two ensembles is created when the detection modes of two samples are overlapped on a single beamsplitter, making it impossible to distinguish between the two sources of idler photons.

All photon-echo quantum memory protocols use a procedure that rephases the atomic dipoles some time later, thereby recreating collective atomic coherence. In other words, the phases of all atoms become equal at some point in time t_e, and this triggers re-emission of the absorbed signal. The initial distribution of spectral detunings δ_j allows for a classification of photon-echo quantum memory into two categories[63]: controlled reversible inhomogenous broadening and atomic frequency combs.

Controlled reversible inhomogeneous broadening. If the spectral distribution is continuous, the requirement of atom-independent phase evolution $\int_0^{t_e} \delta_j(t)dt$ can only be achieved if, some time t' after the absorption of light, the resonance frequency of all atoms is actively changed from δ_{j1} to δ_{j2} such that $\delta_{j1}t' + \delta_{j2}(t_e - t')$ is constant for all values of j (Fig. 4).

This approach to storage can be traced back to 1964, when the well-known spin-echo effect[64] was extended to the optical domain[65]. The two-pulse photon echo was then extended to the time-variable storage

NATURE PHOTONICS DOI: 10.1038/NPHOTON.2009.231

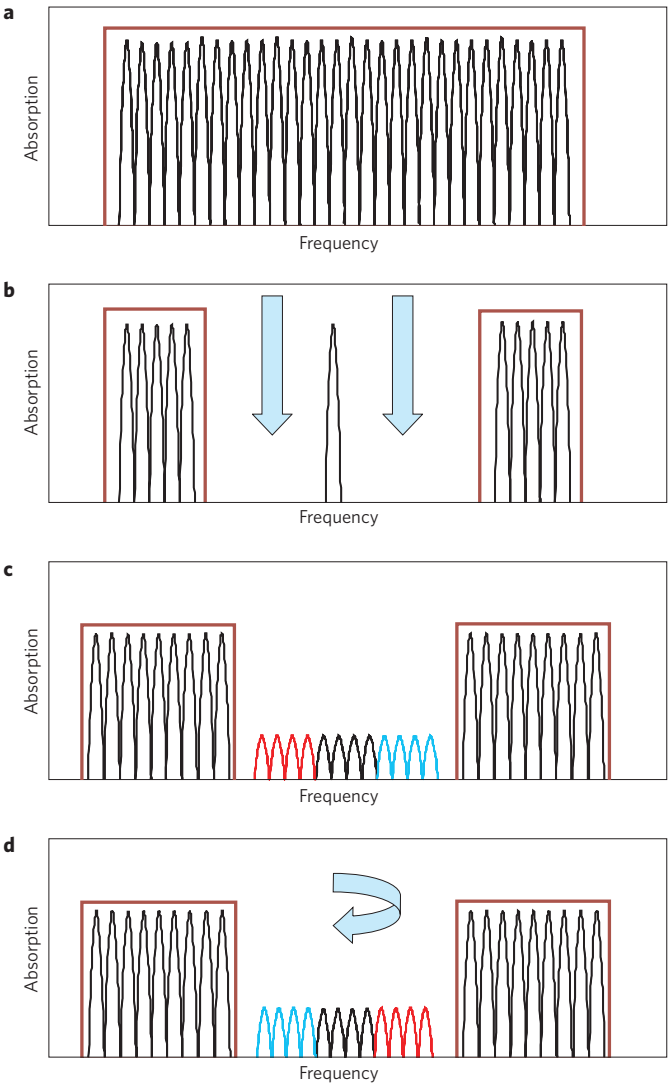

Figure 4 | CRIB-based quantum memory in solid-state devices that feature optical centres with permanent electric dipole moments. **a**, An ensemble of absorbers with broad, inhomogeneously broadened absorption lines. **b**, A narrow absorption line is then created through optical pumping (or spectral hole burning), which transfers population to auxiliary atomic levels. **c**, The line is then broadened in a controlled and reversible way using d.c. Stark shifts and position-dependent external electric fields, causing a reduction in optical depth. The signal to be stored is then directed onto the medium and absorbed. **d**, Re-emission is activated through a mode- or phase-matching operation; that is, it involves a $2kz$-position-dependent phase shift and reversal of the detuning of each atom. This leads to backwards emission of the signal in a time-reversed version. Figures reproduced with permission from ref. 71, © 2009 Wiley-VCH.

of data pulses using three-pulse photon echoes[66–69]. Conventional photon echoes, however, do not allow high-fidelity efficient storage and retrieval of data encoded into few-photon pulses of light, owing to an inherent amplification process[70]. Despite this, conventional photon echoes have recently inspired a quantum memory protocol that is now generally referred to as controlled reversible inhomogeneous broadening (CRIB)[71], also known as gradient echo memory[72]. First proposed in 2001 for storage in atomic vapours[73], CRIB has since been adapted for solid-state storage of microwave[74] and optical photons[75–77].

The original proposal for CRIB is based on hidden time-reversal symmetry in the Maxwell–Bloch equations, which describe the evolution of an atom–light system during absorption and re-emission[77]. Reversing this evolution requires the detuning of all atoms to be inverted; that is, $\delta_{j2} = -\delta_{j1}$. Additionally, a mode- or phase-matching operation must be performed, which consists of applying a phase shift of e^{-2ikzj} to all atoms. This maps the forward-travelling collective atomic coherence — created during absorption of the forward-travelling light — onto a backward-propagating coherence, which can lead to light emission in the backwards direction. Another condition for perfect time-reversal is that the optical depth of the medium must be sufficiently large to guarantee absorption of the incoming light.

If the conditions of atomic inversion, mode-matching and large optical depth are not satisfied, symmetry arguments are not sufficient to predict the memory performance. Cases of particular interest are when the light is not completely absorbed due to limited optical depth, and when the mode-matching operation is not implemented, which results in the light being re-emitted in the forwards direction. To measure the performance, we distinguish between different types of inhomogeneous broadening — two types have been analysed so far. First, in transverse broadening, the atomic absorption line is equally broadened for each position z. Second, in longitudinal broadening, the atomic absorption line for each position z is narrow, and the resonance frequency varies monotonically throughout the medium such that $\delta_j = \chi z_j$, where χ is a proportionality coefficient.

Assuming transverse broadening and a limited optical depth αL, the efficiency for retrieval in the backwards direction is given by[78,79] $\epsilon_b^{(t)} = (1 - \exp(-\alpha L))^2$. For re-emission in the forwards direction, the efficency is[79,80] $\epsilon_f^{(t)} = (\alpha L)^2 \exp(-\alpha L)$, and a maximum efficiency of 54% is obtained for $\alpha L = 2$. It is important to note that the retrieved pulse is time-reversed, resulting in an exchange of the leading and trailing ends, regardless of the direction of retrieval.

Longitudinal broadening yields $\epsilon^{(t)} = \epsilon_f^{(t)} = (1 - \exp(-(\alpha L)_{\text{eff}}))^2$, where $(\alpha L)_{\text{eff}} \propto \chi^{-1}$ and characterizes the effective optical depth of the medium[80–82]. It is interesting that the efficiency for forward retrieval can reach unity despite the violation of time-reversal — although the output pulse is a time-inverted image of the input signal[72], it is re-emitted forwards. The retrieved pulse features a frequency chirp; that is, the fidelity of the retrieved mode is less than unity[81,82].

Depending on the storage medium, the required changes in detuning can be achieved in a number of different ways. For an atomic vapour that has inhomogeneous broadening owing to atomic motion, the atoms are forced to emit light in the backwards direction using the mode-matching operation described above, which inverts the Doppler shifts. In solids, the detuning of the individual atoms depends on the crystal defects and strain. Control over these detunings can be achieved by 'tailoring' a narrow absorption line in the naturally broadened transition — achieved by optical pumping, followed by controlled and reversible broadening through position-dependent Stark or Zeeman shifts (Fig. 4b).

To achieve a large delay–bandwidth product in a two-level system, we require the initial absorption line to be very narrow, which determines the storage time. On the other hand, we also require the broadened line to be very wide, which determines the bandwidth of the pulse to be stored. The requirement of large artificial broadening compromises the optical depth, thereby affecting the storage efficiency, but this can be alleviated by working with broader initial lines and rapidly mapping optical coherence (between levels $|b\rangle$ and $|a\rangle$; Fig. 1a) onto long-lived ground-state coherence (between levels $|b\rangle$ and $|c\rangle$). This transfer can be accomplished using π-pulses or a direct Raman transfer using additional off-resonant control fields that connect levels $|a\rangle$ and $|b\rangle$. If the control fields are counter-propagating, this procedure also implements the mode-matching operation that forces the retrieved signal to propagate backwards.

Photon-echo quantum memory with Raman transfer is sometimes referred to as Raman echo quantum memory[14,63,83–85]. As well as the possibility to work with relatively broad optical absorption lines, this approach may alleviate material requirements because the storage bandwidth depends not only on the controlled inhomogeneous broadening of the optical transition, but also on the Rabi frequency of the Raman control fields[63]. Interestingly, reversible mapping of quantum states between light and atomic ensembles can be obtained for fields of arbitrary strengths — that is, beyond the usual weak-field linear approximation[63].

CRIB was first demonstrated in 2006 using a europium-doped Y_2SiO_5 crystal, a reversible external electric field for generating longitudinal broadening, and macroscopic optical pulses retrieved in the forward direction[76]. As in all photon-echo-based storage, the crystal was cooled to around 4 K. Owing to limited optical depth, the size of the retrieved pulses was six orders of magnitude smaller than that of the input pulses. The same group then demonstrated that amplitude as well as phase information can be stored[86], but (again) with low efficiency. Since then, the memory performance has been improved tremendously, and a record efficiency of 66% was recently reported using a praseodymium-doped Y_2SiO_5 crystal in the configuration above (M. P. Hedges, M. J. Sellars, Y.-M. Lee & J. J. Longdell in a poster presented at *Int. Conf. Hole Burning, Single Molecule and Related Spectroscopies: Science Applications*, 22–27 June 2009).

The europium- and praseodymium-doped crystals used in these experiments have level structures and radiative lifetimes favourable for optical pumping, but have transition frequencies at around 580 nm and 606 nm, respectively. These transitions are inconvenient because they require the use of frequency-stabilized dye lasers. Furthermore, the spectral width of the light to be stored is limited to a few megahertz, owing to the small spacing of atomic levels in the ground and excited state multiplets. Recently, CRIB was implemented using telecommunications-wavelength photons in an erbium-doped Y_2SiO_5 crystal[87]. This material has a more convenient transition at 1,536 nm (allowing standard diode lasers to be used) but it does not provide the same ease-of-use for tailoring the initial absorption line as in europium- or praseodymium-doped Y_2SiO_5. The retrieval efficiency for weak coherent laser pulses was below 1%.

CRIB-based storage was recently combined with a direct Raman transfer[83,85]. The experiments relied on macroscopic signal pulses and storage in rubidium vapour. The first investigation[83] established the feasibility and resulted in a retrieval efficiency of 1%. In the second study[85], efficiency was increased to 41%. By exploiting the condition that pulse emission can only take place if all dipoles oscillate in phase and if the Raman coupling beam is switched on, it was demonstrated that the order and moments of retrieval of four stored pulses can be chosen at will. Hence, the approach could work as an optical random-access memory for quantum information encoded in time-bin qubits. Furthermore, beamsplitting of input pulses was observed, and this has also been demonstrated using EIT systems[42,88–90], traditional stimulated photon echoes[91] and photon-echo quantum memory based on atomic frequency combs (AFCs)[92].

Atomic frequency combs. In this protocol, the distribution of atoms over the detuning δ is described by a periodic comb-like structure that has absorption lines spaced by multiples of Δ (Fig. 5). Repetitive rephasing occurs at times $2\pi/\Delta$, when the phases accumulated by atomic dipoles in different 'teeth' differ by multiples of 2π. To inhibit re-emission after one fixed cycle and to allow for long-term storage with on-demand read-out, the excited optical coherence can be transferred temporarily to coherence between other atomic levels (for example, between ground-state spin levels) where the comb structure is not present. This condition is well satisfied in crystals doped with rare-earth-ions.

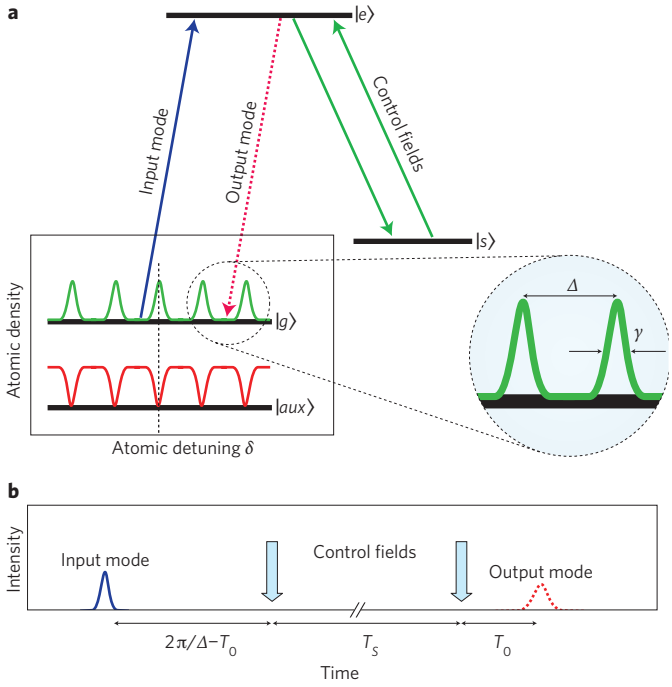

Figure 5 | AFC-based quantum memory. a, An inhomogeneously broadened absorption line (transition $|g\rangle \leftrightarrow |e\rangle$) is prepared in a comb-shaped pattern using frequency-selective optical pumping to the $|aux\rangle$ level. The peaks in the comb are characterized by their width γ and separation Δ. **b**, The collective dipole moment created by absorption of the input light rapidly dephases and, owing to the discrete structure of the absorption profile tailored in **a**, rephases after a time $2\pi/\Delta$. This results in the re-emission of the input light field. The application of a pair of counter-propagating control fields on the $|e\rangle \leftrightarrow |s\rangle$ transition allows for long storage times and efficient on-demand recall in the backwards direction after a storage time T_s. Figures reproduced with permission from ref. 13, © 2009 APS.

The AFC approach originates from the discovery in the late 1970s that photon echoes can be stimulated from accumulated frequency gratings[93–95]. The AFC quantum memory protocol, proposed in 2008[13], is expected to allow time-variable storage of quantum states with unit efficiency and fidelity. Assuming transverse broadening, the efficiency of the AFC protocol can reach 54% and 100% for retrieval in the forward and backward directions, respectively.

Compared with CRIB, AFC has the advantage of making better use of the available optical depth because fewer atoms need to be removed through optical pumping. Another advantage is the unlimited multimode capacity, as long as the natural broadened absorption line is sufficiently large. For instance, calculations suggest the possibility of storing 100 temporal modes with an efficiency of 90% in europium-doped Y_2SiO_5 (ref. 13). For comparison, the multimode capacity in CRIB scales linearly with the absorption depth, and in EIT it is proportional to the square root of the absorption depth[13,14].

In 2008, AFC quantum memory with re-emission after 250 ns — a time predetermined by the spacing in the frequency comb — was reported[91]. The experiment relied on a neodymium-doped YVO_4 crystal and retrieval was in the forward direction. The read-out efficiency was 0.5% for weak coherent input states of ~20-ns duration, and a capacity of up to four temporal modes was demonstrated. The post-selected storage fidelity for time-bin qubits in various states, defined by the average state-overlap, exceeded 97%.

One of the major disadvantages of this scheme — the predetermined emission timing — was overcome recently[96]. For on-demand

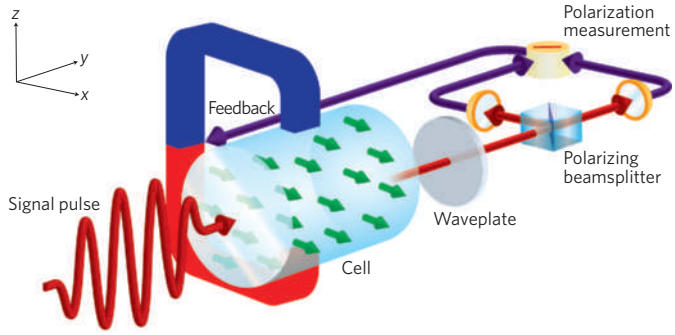

Figure 6 | Quantum memory based on the off-resonant Faraday interaction between light and atoms. Here, quantum information is encoded in the polarization of photons. After propagating through the cell, the pulse is subjected to a polarization measurement, the result of which is then fed back to the atoms by applying a magnetic field pulse of a known magnitude and duration. As a result, the quantum Stokes parameters S_2 and S_3 of the light are mapped onto the angular momentum components J_z and J_y, respectively.

retrieval, the initially excited optical coherence was temporally transferred to ground-state coherence using two π-pulses with a variable relative delay. 450-ns long macroscopic optical pulses were stored in a praseodymium-doped Y_2SiO_5 crystal for up to 20 μs, with an efficiency of around 1%. AFC-based storage was also recently demonstrated in a thulium-doped YAG crystal[97]. Better tailoring of the comb structure resulted in a storage efficiency of 9.1% — an improvement of almost one order of magnitude.

Off-resonant Faraday interaction

Consider an optical wave propagating through an ensemble of two-level atoms. When its detuning Δ from the atomic transition is sufficiently greater than the atomic linewidth, the real part of the susceptibility is inversely proportional to Δ, whereas the imaginary part varies as Δ^{-2} (Fig. 1b,c). An off-resonant wave will therefore not excite any atoms (resulting in negligible absorption) but may experience a significant phase shift. The quantum phase of the atoms will in turn be affected by the field.

This mutual effect between light and atoms can manifest itself in the non-destructive interaction between the optical polarization and the collective atomic angular momentum, which can be utilized to construct an elegant quantum optical memory[98–100]. The scheme was implemented in 2004 by Julsgaard *et al.*[101] using experimental tools that were developed earlier by the same group for the purpose of entangling two atomic ensembles[102].

Consider a signal wave that has macroscopic linear polarization along the *y*-axis; that is, a Stokes parameter of $S_1 = -1$. The quantum information to be stored is encoded in the microscopic Stokes parameters S_2 and S_3 of the wave. The Stokes parameter S_2 is interpreted as the angle of polarization with respect to the *y* axis, whereas S_3 is proportional to the collective spin of the photons.

To implement storage, this field propagates along the *z* direction through an off-resonant atomic gas. The atoms in the gas are initially prepared by optical pumping and have an angular momentum *J* oriented along the *x* axis (Fig. 6). However, because of complementarity, the atomic angular momentum must have a spread along the *z*- and *y*-axes.

This scheme relies on two complementary effects. First, the *z* component of the atomic angular momentum causes Faraday rotation, which changes S_2. Second, the atoms precess around the *z* axis because of the photons' spin S_3, which affects the J_y component of the atomic angular momentum. In this way, some of the quantum information carried by the light is transferred to the atoms and vice versa.

To complete the memory protocol, we then perform a polarization measurement on the pulse emerging from the atomic ensemble, thereby determining its Stokes parameter S_2. We then perform a feedback operation on the atoms by applying a magnetic field — the magnitude and direction of which is determined by the measurement read-out — along the *y* axis. Precession of the atoms about the magnetic field affects the *z* component of their angular momentum. Thus, the initial Stokes parameter S_2 of the photons is mapped onto J_z of the atoms.

This results in both components of the optical polarization being transferred to the atomic angular momentum. Although the J_y component is still 'contaminated' by its initial uncertainty, this imperfection can be eliminated by initially preparing the atoms in the spin-squeezed state[103,104]. In the study of Julsgaard *et al.*[101], the atoms were prepared without initial spin squeezing. However, the apparatus was shown to beat the classical benchmark[12] for coherent states of mean energies up to ten photons with a storage time of 4 ms. This experiment was the first demonstration of the quantum properties of an optical memory.

Theoretical proposals[98,99] describe a set-up that involves passing the light through the atomic ensemble twice — in two different directions — to eliminate both the measurement and feedback proceedures in the scheme described above, but this has not yet been implemented experimentally.

Lifetime and decoherence

A common feature of all approaches to quantum memory through atom–light interactions is the storage of information in a collective atomic coherence. All methods are therefore prone to decoherence, which limits the storage time.

In the case of CRIB and AFC, the storage time is also affected by the width of the tailored absorption lines (Fig. 4a) as long as information is stored coherently between the ground and the optically excited states[79]. This width is fundamentally limited by the intrinsic homogeneous linewidth of the optical transition[71,105–109], and practically limited by laser line fluctuations and power broadening during optical pumping. Decoherence can be reduced by temporally mapping the optical coherence onto coherence between ground states, which are generally associated with smaller linewidths and longer coherence times[96].

The storage time in Raman-type memory, including in EIT, DLCZ and Raman echo quantum memory, is limited by ground-state decoherence. For instance, in vapour cells, the leading source of ground-state decoherence is the drift of atoms in and out of the laser beam. To reduce this effect, cells with inert buffer gases and/or paraffin-coated walls are generally used together with geometrically wider optical modes. In ultracold atoms confined to magneto-optical traps, decoherence often comes from the magnetic field. This field produces a non-uniform Zeeman shift of atomic ground levels, leading to a loss of quantum phase in collective superpositions.

Significant improvements to the memory lifetimes of atomic ensembles has recently been reported in two DLCZ experiments[110,111]. The effect of the magnetic field has been minimized by using the atomic 'clock' states — magnetic sublevels whose two-photon detuning is minimally affected by the Zeeman effect — as the ground states of the system. Zhao *et al.* have eliminated residual atomic motion[111] by transferring the atoms from a magneto-optical trap to an optical lattice of a sufficiently small period, and Schnorrberger *et al.*[110] instead used a collinear geometry for the four optical fields involved (in this case the dephasing due to atomic motion becomes insignificant). In both experiments, storage times over a millisecond have been reported.

Very recently[112], EIT-based storage of light has been demonstrated in an atomic Mott insulator — a collection of atoms filling a three-

dimensional optical lattice, with one atom per lattice site. Absence of mechanical motion and uniformity of the magnetic field resulted in a storage lifetime of 238 ms, which is the current record for atomic media. The residual ground-state coherence decay probably results from heating in the optical lattice, and also from atomic tunnelling.

Coherence lifetimes even longer than this can be achieved in crystals doped with rare-earth ions. Decoherence mechanisms vary depending on the crystal and dopant. For instance, the dominant mechanism in praseodymium-doped Y_2SiO_5 crystals is random Zeeman shifting of Pr^{3+} ions, which results from the fluctuating magnetic fields of yttrium nuclei. Fortunately, this effect can be significantly reduced by operating in a uniform magnetic field of certain magnitude and direction. Through this approach, coherence times of up to 82 ms have been reported[113]. This was further increased to 30 s by introducing dynamic decoherence control[114].

Conclusions

Quantum memory for light constitutes a promising, rapidly developing research topic that builds on decades of research into atomic spectroscopy, quantum optics and materials science. Recent results show efficient storage with high fidelity, high multimode capacities and long lifetimes with on-demand retrieval. However, these performance characteristics have so far been demonstrated using different storage media and protocols, and more effort is required to combine these benchmarks in a single set-up. When achieved, such a device will be invaluable for quantum communication and cryptography, as well as for optical quantum computation.

References

1. Gisin, N., Ribordy, G., Tittel, W. & Zbinden, H. Quantum cryptography. *Rev. Mod. Phys.* **74,** 145–195 (2002).
2. Mermin, N. D. *Quantum Computer Science* Ch. 3 (Cambridge Univ. Press, 2007).
3. Lloyd, S. Universal quantum simulators. *Science* **273,** 1073–1078 (1996).
4. Knill, E., Laflamme, R. & Milburn, G. J. A scheme for efficient quantum computation with linear optics. *Nature* **409,** 46–52 (2001).
5. Lund, A. P. & Ralph, T. C. Nondeterministic gates for photonic single-rail quantum logic. *Phys. Rev. A* **66,** 032307 (2002).
6. Berry, D. W., Lvovsky, A. I. & Sanders, B. C. Interconvertibility of single-rail optical qubits. *Opt. Lett.* **31,** 107–109 (2006).
7. Marcikic, I. *et al.* Time-bin entangled qubits for quantum communication created by femtosecond pulses. *Phys. Rev. A* **66,** 062308 (2002).
8. Gottesman, D. in *Encyclopedia of Mathematical Physics* Vol. 4, (eds Francoise, J.-P., Naber, G. L. & Tsou, S. T.) 196–201 (Elsevier, 2006).
9. Shor, P. W. Scheme for reducing decoherence in quantum computer memory. *Phys. Rev. A* **52,** R2493–R2496 (1995).
10. Lobino, M. *et al.* Complete characterization of quantum–optical processes. *Science* **322,** 563–566 (2008).
11. Lobino, M., Kupchak, C., Figueroa, E. & Lvovsky A. I. Memory for light as a quantum process. *Phys. Rev. Lett.* **102,** 203601 (2009).
12. Hammerer, K., Polzik, E. S. & Cirac, J. I. Teleportation and spin squeezing utilizing multimode entanglement of light with atoms. *Phys. Rev. A* **72,** 052313 (2005).
13. Afzelius, M., Simon, C., de Riedmatten, H. & Gisin, N. Multimode quantum memory based on atomic frequency combs. *Phys. Rev. A* **79,** 052329 (2009).
14. Nunn, J. *et al.* Multimode memories in atomic ensembles. *Phys. Rev. Lett.* **101,** 260502 (2008).
15. Raussendorf, R. & Briegel, H. J. A one-way quantum computer. *Phys. Rev. Lett.* **86,** 5188–5191 (2001).
16. Kok, P. *et al.* Linear optical quantum computing with photonic qubits. *Rev. Mod. Phys.* **79,** 135–174 (2007).
17. Briegel, H.-J., Dür, W., Cirac, J. I. & Zoller, P. Quantum repeaters: The role of imperfect local operations in quantum communication. *Phys. Rev. Lett.* **81,** 5932–5935 (1998).
18. Sangouard, M., Simon, C., de Riedmatten, H. & Gisin, N. Quantum repeaters based on atomic ensembles and linear optics. Preprint at <http://arxiv.org/abs/0906.2699> (2009).
19. Appel, J. *et al.* Mesoscopic atomic entanglement for precision measurements beyond the standard quantum limit. *Proc. Natl Acad. Sci. USA* **106,** 10960–10965 (2009).
20. Hong, C. K. & Mandel, L. Experimental realization of a localized one-photon state. *Phys. Rev. Lett.* **56,** 58–60 (1986).
21. Grangier, P., Roger, G. & Aspect, A. Experimental evidence for a photon anticorrelation effect on a beam splitter: a new light on single-photon interferences. *Europhys. Lett.* **1,** 173–179 (1986).
22. Landry, O., van Houwelingen, J. A. W., Beveratos, A., Zbinden, H. & Gisin, N. Quantum teleportation over the Swisscom telecommunication network. *J. Opt. Soc. Am. B* **24,** 398–403 (2007).
23. Pittman, T. B., Jacobs, B. C. & Franson, J. D. Single Photons on pseudodemand from stored parametric down-conversion. *Phys. Rev. A* **66,** 042303 (2002).
24. Pittman, T. B. & Franson, J. D. Cyclical quantum memory for photonic qubits. *Phys. Rev. A* **66,** 062302 (2002).
25. Leung, P. M. & Ralph, T. C. Quantum memory scheme based on optical fibres and cavities. *Phys. Rev. A* **74,** 022311 (2006).
26. Maître, X. *et al.* Quantum memory with a single photon in a cavity. *Phys. Rev. Lett.* **79,** 769–772 (1997).
27. Tanabe, T., Notomi, M., Kuramochi, E., Shinya, A. & Taniyama, H. Trapping and delaying photons for one nanosecond in an ultrasmall high-*Q* photonic-crystal nanocavity. *Nature Photon.* **1,** 49–52 (2007).
28. Tanabe, T., Notomi, M., Taniyama, H. & Kuramochi, E. Dynamic release of trapped light from an ultrahigh-*Q* nanocavity via adiabatic frequency tuning. *Phys. Rev. Lett.* **102,** 043907 (2009).
29. Javan, A., O. Kocharovskaya, Lee, H. & Scully, M. O. Narrowing of electromagnetically induced transparency resonance in a Doppler-broadened medium. *Phys. Rev. A* **66,** 013805 (2002).
30. Kasapi, A., Jain, M., Yin, G. Y. & Harris, S. E. Electromagnetically induced transparency: Propagation dynamics. *Phys. Rev. Lett.* **74,** 2447–2450 (1995).
31. Fleischhauer, M. & Lukin, M. D. Quantum memory for photons: Dark-state polaritons. *Phys. Rev. A* **65,** 022314 (2002).
32. Budker, D., Kimball, D. F., Rochester, S. M. & Yashchuk, V. V. Nonlinear magneto-optics and reduced group velocity of light in atomic vapor with slow ground state relaxation. *Phys. Rev. Lett.* **83,** 1767–1770 (1999).
33. Hau, L. V., Harris, S. E., Dutton, Z. & Behroozi, C. H. Light speed reduction to 17 metres per second in an ultracold atomic gas. *Nature* **397,** 594–598 (1999).
34. Fleischhauer, M. & Lukin, M. D. Dark-state polaritons in electromagnetically induced transparency. *Phys. Rev. Lett.* **84,** 5094–5097 (2000).
35. Lukin, M. D. Colloquium: Trapping and manipulating photon states in atomic ensembles. *Rev. Mod. Phys.* **75,** 457–472 (2003).
36. Fleischhauer, M., Imamoglu, A. & Marangos, J. P. Electromagnetically induced transparency: Optics in coherent media. *Rev. Mod. Phys.* **77,** 633–673 (2005).
37. Phillips, D. F., Fleischhauer, A., Mair, A., Walsworth, R. L. & Lukin, M. D. Storage of light in atomic vapor. *Phys. Rev. Lett.* **86,** 783–786 (2001).
38. Liu, C., Dutton, Z., Behroozi, C. H. & Hau, L. V. Observation of coherent optical information storage in an atomic medium using halted light pulses. *Nature* **409,** 490–493 (2001).
39. Gorshkov, A. V., André, A., Fleischhauer, M., Sørensen, A. S. & Lukin, M. D. Universal approach to optimal photon storage in atomic media. *Phys. Rev. Lett.* **98,** 123601 (2007).
40. Phillips, N. B., Gorshkov, A. V. & Novikova, I. Optimal light storage in atomic vapor. *Phys. Rev. A* **78,** 023801 (2008).
41. Novikova, I. *et al.* Optimal control of light pulse storage and retrieval. *Phys. Rev. Lett.* **98,** 243602 (2007).
42. Novikova, I., Phillips, N. B. & Gorshkov, A. V. Optimal light storage with full pulse-shape control. *Phys. Rev. A* **78,** 021802(R) (2008).
43. Camacho, R. M., Vudyasetu, P. K. & Howell, J. C. Four-wave-mixing stopped light in hot atomic rubidium vapour. *Nature Photon.* **3,** 103–106 (2009).
44. Ichimura, K., Yamamoto, K. & Gemma, N. Evidence for electromagnetically induced transparency in a solid medium. *Phys. Rev. A* **58,** 4116–4120 (1998).
45. Turukhin, A. V. *et al.* Observation of ultraslow and stored light pulses in a solid. *Phys. Rev. Lett.* **88,** 023602 (2001).
46. Longdell, J. J., Fraval, E., Sellars, M. J. & Manson, N. B. Stopped light with storage times greater than one second using electromagnetically induced transparency in a solid. *Phys. Rev. Lett.* **95,** 063601 (2005).
47. Goldner, P. *et al.* Long coherence lifetime and electromagnetically induced transparency in a highly-spin-concentrated solid. *Phys. Rev. A* **79,** 033809 (2009).
48. Chanelière, T. *et al.* Storage and retrieval of single photons transmitted between remote quantum memories. *Nature* **438,** 833–836 (2005).
49. Eisaman, M. D. *et al.* Electromagnetically induced transparency with tunable single-photon pulses. *Nature* **438,** 837–841 (2005).
50. Choi, K. S., Deng, H., Laurat, J. & Kimble, H. J. Mapping photonic entanglement into and out of a quantum memory. *Nature* **452,** 67–71 (2008).
51. Akamatsu, D., Akiba, K. & Kozuma, M. Electromagnetically induced transparency with squeezed vacuum. *Phys. Rev. Lett.* **92,** 203602 (2004).
52. Honda, K. *et al.* Storage and retrieval of a squeezed vacuum. *Phys. Rev. Lett.* **100,** 093601 (2008).

53. Arikawa, M. *et al.* Quantum memory of a squeezed vacuum for arbitrary frequency sidebands. Preprint at <http://arxiv.org/abs/0905.2816> (2009).
54. Appel, J., Figueroa, E., Korystov, D., Lobino, M. & Lvovsky, A. I. Quantum memory for squeezed light. *Phys. Rev. Lett.* **100,** 093602 (2008).
55. Figueroa, E., Vewinger, F., Appel, J. & Lvovsky, A. I. Decoherence of electromagnetically induced transparency in atomic vapor. *Opt. Lett.* **31,** 2625–2627 (2006).
56. Hsu, M. T. L. *et al.* Quantum study of information delay in electromagnetically induced transparency. *Phys. Rev. Lett.* **97,** 183601 (2006).
57. Peng, A. *et al.* Squeezing and entanglement delay using slow light. *Phys. Rev. A* **71,** 033809 (2005).
58. Hétet, G. *et al.* Erratum: Squeezing and entanglement delay using slow light. *Phys. Rev. A* **74,** 059902(E) (2006).
59. Hétet, G., Peng, A., Johnsson, M. T., Hope, J. J. & Lam, P. K. Characterization of electromagnetically-induced-transparency-based continuous-variable quantum memories. *Phys. Rev. A* **77,** 012323 (2008).
60. Figueroa, E., Lobino, M., Korystov, D., Appel, J. & Lvovsky, A. I. Propagation of squeezed vacuum under electromagnetically induced transparency. *New J. Phys.* **11,** 013044 (2009).
61. Duan, L.-M., Lukin, M. D., Cirac, J. I. & Zoller, P. Long-distance quantum communication with atomic ensembles and linear optics. *Nature* **414,** 413–418 (2001).
62. Chen, Y.-A. *et al.* Memory-build-in quantum teleportation with photonic and atomic qubits. *Nature Phys.* **4,** 103–107 (2008).
63. Moiseev, S. A. & Tittel, W. Optical quantum memory with generalized time-reversible atom–light interactions. Preprint at <http://arxiv.org/abs/0812.1730> (2009).
64. Hahn, E. L. Spin echoes. *Phys. Rev.* **80,** 580–594 (1950).
65. Kurnit, N. A., Abella, I. D. & Hartmann, S. R. Observation of a photon echo. *Phys. Rev. Lett.* **13,** 567–568 (1964).
66. Elyutin, S. O., Zakharov, S. M. & Manykin, E. A. Theory of formation of photon echo pulses. *Sov. Phys. JETP* **49,** 421–431 (1979).
67. Mossberg, T. W. Time-domain frequency-selective optical data storage. *Opt. Lett.* **7,** 77–79 (1982).
68. Mossberg, T., Flusberg, A., Kachru, R. & Hartmann, S. R. Total scattering cross section for Na on He measured by stimulated photon echoes. *Phys. Rev. Lett.* **42,** 1665–1669 (1979).
69. Carlson, N. W., Rothberg, L. J., Yodh, A. G., Babbitt, W. R. & Mossberg, T. W. Storage and time reversal of light pulses using photon echoes. *Opt. Lett.* **8,** 483–485 (1983).
70. Ruggiero, J., Le Gouët, J.-L, Simon, C. & Chanelière, T. Why the two-pulse photon echo is not a good quantum memory protocol. *Phys. Rev. A* **79,** 053851 (2009).
71. Tittel, W. *et al.* Photon-echo quantum memory in solid state systems. *Laser Photon. Rev.* doi:10.1002/lpor.200810056 (2009).
72. Hétet, G., Longdell, J. J., Sellars, M. J., Lam, P. K. & Buchler, B. C. Multimodal properties and dynamics of gradient echo quantum memory. *Phys. Rev. Lett.* **101,** 203601 (2008).
73. Moiseev, S. A. & Kröll, S. Complete reconstruction of the quantum state of a single-photon wave packet absorbed by a Doppler-broadened transition. *Phys. Rev. Lett.* **87,** 173601 (2001).
74. Moiseev, S. A., Tarasov, V. F. & Ham, B. S. Quantum memory photon echo-like techniques in solids. *J. Opt. B* **5,** S497–S502 (2003).
75. Nilsson, M. & Kröll, S. Solid state quantum memory using complete absorption and re-emission of photons by tailored and externally controlled inhomogeneous absorption profiles. *Opt. Commun.* **247,** 393–403 (2005).
76. Alexander, A. L., Longdell, J. J., Sellars, M. J. & Manson, N. B. Photon echoes produced by switching electric fields. *Phys. Rev. Lett.* **96,** 043602 (2006).
77. Kraus, B. *et al.* Quantum memory for nonstationary light fields based on controlled reversible inhomogeneous broadening. *Phys. Rev. A* **73,** 020302(R) (2006).
78. Moiseev, S. A. & Noskov, M. I. The possibilities of the quantum memory realization for short pulses of light in the photon echo technique. *Laser Phys. Lett.* **1,** 303–310 (2004).
79. Sangouard, N., Simon, C., Afzelius, M. & Gisin, N. Analysis of a quantum memory for photons based on controlled reversible inhomogeneous. broadening. *Phys. Rev. A* **75,** 032327 (2007).
80. Longdell, J. J., Hétet, G., Lam, P. K. & Sellars, M. J. Analytic treatment of controlled reversible inhomogeneous broadening quantum memories for light using two-level atoms. *Phys. Rev. A* **78,** 032337 (2008).
81. Hétet, G., Longdell, J. J., Alexander, A. L., Lam, P. K. & Sellars, M. J. Electro-optic quantum memory for light using two-level atoms. *Phys. Rev. Lett.* **100,** 023601 (2008).
82. Moiseev, S. A. & Arslanov, N. M. Efficiency and fidelity of photon-echo quantum memory in an atomic system with longitudinal inhomogeneous broadening. *Phys. Rev. A* **78,** 023803 (2008).
83. Hétet, G. *et al.* Photon echoes generated by reversing magnetic field gradients in a rubidium vapor. *Opt. Lett.* **33,** 2323–2325 (2008).
84. Le Gouët, J.-L. & Berman, P. R. Raman scheme for adjustable-bandwidth quantum memory. *Phys. Rev. A* **80,** 012320 (2009).
85. Hosseini, M. *et al.* Coherent optical pulse sequencer for quantum applications. *Nature* **461,** 241–245 (2009).
86. Alexander, A. L., Longdell, J. J., Sellars, M. J. & Manson, N. B. Coherent information storage with photon echoes produced by switching electric fields. *J. Lumin.* **127,** 94–97 (2007).
87. Lauritzen, B. *et al.* Solid state quantum memory for photons at telecommunication wavelengths. Preprint at <http://arxiv.org/abs/0908.2348> (2009).
88. Appel, J., Marzlin, K.-P. & Lvovsky, A. I. Raman adiabatic transfer of optical states in multilevel atoms. *Phys. Rev. A* **73,** 013804 (2006).
89. Vewinger, F., Appel, J., Figueroa, E. & Lvovsky, A. I. Adiabatic frequency conversion of quantum optical information in atomic vapor. *Opt. Lett.* **32,** 2771–2773 (2007).
90. Campbell, G., Ordog, A. & Lvovsky, A. I. Multimode electromagnetically induced transparency on a single atomic line. *New J. Phys.* **11,** 103021 (2009).
91. Staudt, M. U. *et al.* Investigations of optical coherence properties in an erbium-doped silicate fiber for quantum state storage. *Opt. Commun.* **266,** 720–726 (2006).
92. de Riedmatten, H., Afzelius, M., Staudt, M. U., Simon, C. & Gisin, N. A solid-state light–matter interface at the single-photon level. *Nature* **456,** 773–777 (2008).
93. Hesselink, W. H. & Wiersma, D. A. Picosecond photon echoes stimulated from an accumulated grating. *Phys. Rev. Lett.* **43,** 1991–1994 (1979).
94. Rebane, A., Kaarli, R., Saari, P., Anijalg, A. & Timpmann, K. Photochemical time-domain holography of weak picosecond pulses. *Opt. Commun.* **47,** 173–176 (1983).
95. Mitsunaga, M., Yano, R. & Uesugi, N. Spectrally programmed stimulated photon echo. *Opt. Lett.* **16,** 264–266 (1991).
96. Afzelius, M. *et al.* Demonstration of atomic frequency comb memory for light with spin-wave storage. Preprint at <http://arxiv.org/abs/0908.2309> (2009).
97. Chanelière, T., Ruggiero, J., Bonarota, M., Afzelius, M. & Le Gouët, J.-L. Efficient light storage in a crystal using an atomic frequency comb. Preprint at <http://arxiv.org/abs/0902.2048> (2009).
98. Kuzmich, A. & Polzik, E. S. in *Quantum Information with Continuous Variables* (eds Braunstein, S. L. & Pati, A. K.) 231–265 (Kluwer, 2003).
99. Muschik, C. A., Hammerer, K., Polzik, E. S. & Cirac, J. I. Efficient quantum memory and entanglement between light and an atomic ensemble using magnetic fields. *Phys. Rev. A* **73,** 062329 (2006).
100. Hammerer, K., Sørensen, A. S. & Polzik, E. S. Quantum interface between light and atomic ensembles. Preprint at <http://arxiv.org/abs/0807.3358> (2009).
101. Julsgaard, B., Sherson, J., Cirac, J. I., Fiurášek, J. & Polzik, E. S. Experimental demonstration of quantum memory for light. *Nature* **432,** 482–486 (2004).
102. Julsgaard, B., Kozhekin, A. & Polzik, E. S. Experimental long-lived entanglement of two macroscopic objects. *Nature* **413,** 400–403 (2001).
103. Kitagawa, M. & Ueda, M. Squeezed spin states. *Phys. Rev. A* **47,** 5138–5143 (1993).
104. Kuzmich, A., Bigelow, N. P. & Mandel, L. Atomic quantum non-demolition measurements and squeezing. *Europhys. Lett.* **42,** 481–486 (1998).
105. Macfarlane, R. M. & Shelby, R. M. in *Spectroscopy of Solids Containing Rare Earth Ions* (eds Kaplyanskii, A. A. & Macfarlane, R. M.) (North-Holland, 1987).
106. Macfarlane, R. M. High-resolution laser spectroscopy of rare-earth doped insulators: a personal perspective. *J. Lumin.* **100,** 1–20 (2002).
107. Sun, Y., Thiel, C. W., Cone, R. L., Equall, R. W. & Hutcheson, R. L. Recent progress in developing new rare earth materials for hole burning and coherent transient applications. *J. Lumin.* **98,** 281–287 (2002).
108. Liu, G. & Jacquier, B. *Spectroscopic Properties of Rare Earths in Optical Materials* (Springer, 2005).
109. Macfarlane, R. M. Optical Stark spectroscopy of solids. *J. Lumin.* **125,** 156–174 (2007).
110. Zhao, B. *et al.* A millisecond quantum memory for scalable quantum networks. *Nature Phys.* **5,** 95–99 (2008).
111. Zhao, R. *et al.* Long-lived quantum memory. *Nature Phys.* **5,** 100–104 (2008).
112. Schnorrberger, U. *et al.* Electromagnetically induced transparency and light storage in an atomic Mott insulator. *Phys. Rev. Lett.* **103,** 033003 (2009).
113. Fraval, E., Sellars, M. J. & Longdell, J. J. Method of extending hyperfine coherence times in Pr^{3+}:Y_2SiO_5. *Phys. Rev. Lett.* **92,** 077601 (2004).
114. Fraval, E., Sellars, M. J. & Longdell, J. J. Dynamic decoherence control of a solid-state nuclear-quadrupole qubit. *Phys. Rev. Lett.* **95,** 030506 (2005).

Acknowledgements

This work was supported by iCORE, QuantumWorks, NSERC, CFI and GDC. A.I.L. is a CIFAR Scholar and B.C.S. is a CIFAR Associate.